Transactions of the Materials Research Society of Japan 30[3] 789-792 (2005)

Blister Formation in Rutile TiO_2 (100) Thin Films by Helium Ion Implantation

Shunya Yamamoto, Shinji Nagata*, Akinori Takayama, Masahito Yoshikawa
Japan Atomic Energy Research Institute, Department of Material Development, 1233 Watanuki, Takasaki Gunma 370-1292, Japan
Fax: 81-27-346-9687, e-mail: yamamoto@taka.jaeri.go.jp
*Tohoku University, Institute for Materials Research, 2-1-1 Katahira, Aoba-ku, Sendai 980-8577, Japan

The photocatalytic properties of titanium dioxide (TiO_2) have attracted much interest from the viewpoints of basic science and applications. For improving photocatalytic activity of TiO_2 films, modification of surface features and fabrication of effective large surface area was required. In this study, implantation energy and fluences of helium ion for blister formation in epitaxial rutile TiO_2 (100) films was investigated. High-quality epitaxial TiO_2 (100) thin films with 500 nm thickness were grown on α-Al_2O_3 (0001) substrates by pulsed laser deposition (PLD) using a KrF excimer laser in an O_2 atmosphere. The TiO_2 films were implanted at room temperature with 1~4 keV helium ions up to fluence range from 1×10^{16} to 2.3×10^{17} ions/cm^2. The surface morphology of TiO_2 films was observed by scanning electron microscope (SEM) with a field-emission gun and atomic force microscope (AFM). Rutherford backscattering spectroscopy (RBS) with channeling was used to determine the radiation-induced damage depth profile near the surface region. Helium blisters with about 100 nm size in TiO_2 films were observed at 2~4 keV helium ion fluences higher than 4×10^{16} ions/cm^2. With further increase of implantation fluences higher than 2×10^{17} ions/cm^2, exfoliation of flakes of the TiO_2 film was observed.

Key words: Helium, Blister, TiO_2, SEM, AFM, RBS

1. INTRODUCTION

The photocatalytic properties of titanium dioxide (TiO_2) have attracted much interest from the viewpoints of basic science and applications. Especially interesting is the photocatalytic property [1], and it can be utilized to decompose toxic gases into safe gaseous compounds using solar energy [2]. TiO_2 is known to crystallize in three different crystallographic structures: rutile (tetragonal), anatase (tetragonal) and brookite (orthorhombic), and the rutile, which is most stable, has been extensively studied and widely used. Several works were reported about epitaxial rutile and anatase films by metal-organic chemical vapor deposition [3], ion beam sputtering [4, 5], and pulsed laser deposition (PLD) [6-9]. For improving photocatalytic activity of TiO_2 films, the control of crystal quality and the fabrication of effective large surface area are required.

The implantation of helium into materials can be used to produce specific microstructures on surface region, such as bubbles, blisters and craters, with unique properties for application such as catalysis [10-13]. These structures have potential for increasing effective surface area and improving photocatalytic activity. The formation of helium bubbles and blisters in materials is a complex phenomenon depending on the helium implantation energy and fluence, implantation temperature and post thermal treatments.

In the present study, we explore the suitable condition for helium blister formation in epitaxial TiO_2 film by helium implantation at room temperature. The observation of helium blisters in film surface was made with scanning electron microscope (SEM) and atomic force microscope (AFM). The optimal implantation condition for the blister formation, helium implantation energy and fluence are reported.

2. EXPERIMENTAL

TiO_2 films were deposited on α-Al_2O_3 substrates by PLD using a KrF excimer laser (wavelength: 248 nm, Lambda Physik). The laser beam was incident on a target with an incident angle of 45°. It was focused to a 2 mm × 3 mm rectangle on a single-crystal TiO_2 (rutile type) target (ϕ35 mm). Typical laser energy and repetition rate were 150 mJ/cm^2 and 5 Hz. Both the target stage and substrate holder were rotated during the deposition. The substrates were separated by about 5 cm from the target. The deposition chamber was evacuated up to a base pressure of about 6×10^{-4} Pa using a turbo-molecular pump (TMP). Oxygen gas (purity: 4N) was flowed into the chamber through a mass-flow meter controlled by an absolute pressure gauge (Baratron 626, MKS) under the pumping

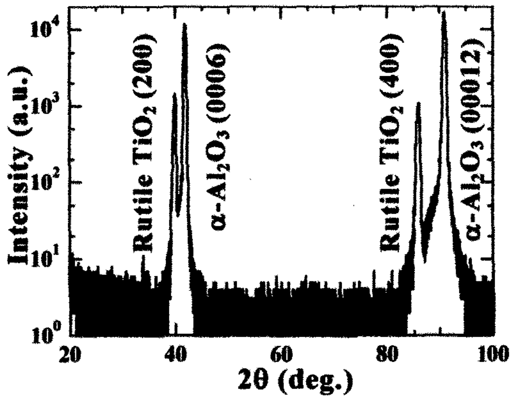

Fig. 1. X-ray diffraction pattern for TiO_2 films on the α-Al_2O_3 (0001) substrate. TiO_2 film was deposited at 500 °C under the oxygen pressure of 2 Pa by PLD.

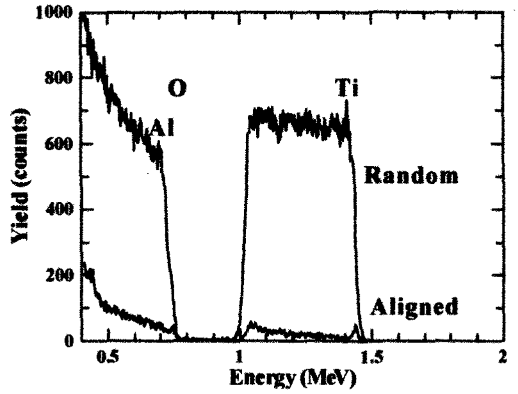

Fig. 2. 2.0 MeV $^4He^+$ RBS/channeling spectra for deposited TiO_2 films on the α-Al_2O_3 (0001) substrate. The thickness of TiO_2 film is 500 nm. The aligned spectrum was taken with the beam directed along the <100> axis of the TiO_2 film.

condition. Single-crystal α-Al_2O_3 (0001) substrates were obtained commercially. They are mirror-polished at both sides, and the typical size is 10 × 10 × 0.3 mm^3. In this study, ~500 nm thick TiO_2 films were deposited at 500 °C under oxygen pressure of 2 Pa.

The deposited TiO_2 films were implanted at room temperature with 1~4 keV helium ions up to fluence range from 1×10^{16} to 2.3×10^{17} ions/cm^2. Implantation of helium ions was carried out using a 4 keV ion gun. The irradiation chamber was evacuated up to a base pressure of about 3.7×10^{-6} Pa using a TMP. Helium gas (purity: 6N) was introduced up to 3.0×10^{-4} Pa during the implantation. The beam current density was 1 μA/cm^2 through a circular slit with 5.5 mm in diameter.

The surface morphology of the deposited films, an important factor for the photocatalytic activities, was examined using a high-resolution field emission SEM (JSM6700F, JEOL) and AFM (SPA400, SII). The crystal structure of TiO_2 films was determined by X-ray diffraction measurements using a high-resolution diffractometer (X'Pert-MRD, PANalytical). Rutherford backscattering spectroscopy (RBS)/channeling analysis using a 3 MV single-stage-accelerator at JAERI/Takasaki was employed to characterize the epitaxial thin films. The analyzing 2.0 MeV $^4He^+$ ions were incident and backscattered particles were detected at 165° scattering angle with a surface barrier detector. Samples were mounted on a 3-axis goniometer to pattern the planar channeling and the axial channeling in the angular coordinate. The film thickness and composition were evaluated from RBS spectra.

3. RESULTS AND DISCUSSION

The suitable condition for high quality epitaxial TiO_2 (100) films with rutile type was following conditions; laser energy: 150 mJ/cm^2, oxygen gas pressures: 2 Pa, substrate temperature: 500°C, target species: single-crystal TiO_2 (rutile type). Figure 1 shows the typical θ–2θ X-ray diffraction pattern for TiO_2 film on the α-Al_2O_3 (0001) substrate. It can be seen from Fig. 1, only the (100) reflections from the TiO_2 are observed without any reflection from the substrates, which indicates that the TiO_2 film is grown with (100) orientation. The pole figure studies in the TiO_2 (100) film on α-Al_2O_3 (0001) indicate that this film consists of three domains rotated 120° each other around TiO_2 <100> growth direction.

The quality of epitaxial TiO_2 (100) films was characterized through the RBS/channeling analysis. Figure 2 illustrates 2.0 MeV $^4He^+$ RBS spectra for the TiO_2 film on the α-Al_2O_3 (0001)

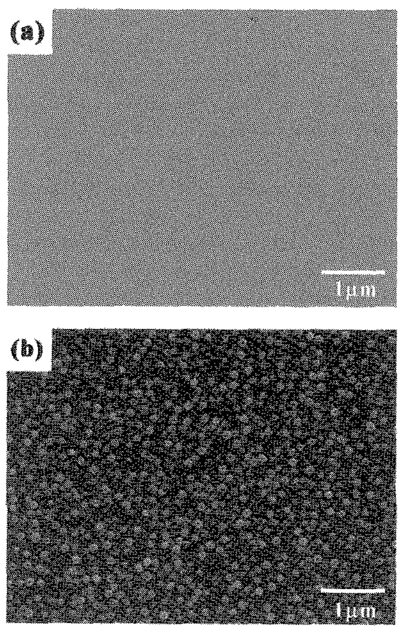

Fig. 3. SEM images of the TiO_2 (100) film (a) unimplanted region and (b) implanted with 3 keV helium ions at room temperature. The TiO_2 film was implanted with the helium fluence of 2.0×10^{17} ions/cm^2.

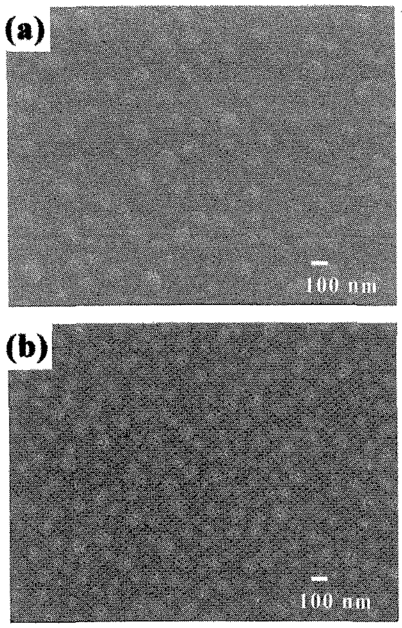

Fig. 4. SEM images of the TiO_2 (100) films implanted with the helium fluence of (a) 1.8 × 10^{17} ions/cm^2 and (b) 2.3 × 10^{17} ions/cm^2. The film samples were implanted with 3 keV helium ions at room temperature.

substrate taken under the random and the axial channeling condition. The aligned spectrum was taken with the beam directed along the <100> axis of the TiO_2 film. The RBS spectra in Fig. 2, one can recognize clearly the separated peaks from the TiO_2 film and α-Al_2O_3 substrate. The peaks at 1.45 MeV correspond to the Ti component in the TiO_2 film. Judging from the peak intensity, the high quality TiO_2 film is grown up from the interface and the interface is not mixed with each other within the depth resolution (~10 nm) of this technique. The minimum yield, χ_{min} value, the ratio between the random and the axially aligned yield at the fixed depth near the surface region, gives a measure to evaluate the degree of disorder in crystalline solids. The χ_{min} value in the <100> aligned spectrum is 0.02 at the just area behind the surface peak of the Ti component in the TiO_2 film, which suggests that the crystal quality of the TiO_2 film is high enough as in a bulk single-crystal. The planar channeling analysis around the major axes of the TiO_2 film and the α-Al_2O_3 gives the evidence that the TiO_2 <100> crystallographic axis is parallel to the α-Al_2O_3 <0001> axis.

SEM images of the TiO_2(100) film unimplanted and implanted with 3 keV helium ions at room temperature are shown in Fig. 3 (a) and (b), respectively. The TiO_2 film was implanted with the helium fluence of 2.0 × 10^{17} ions/cm^2. It can be seen from Fig. 3 (a), smooth surface structure is observed in unimplanted region of the film. In Fig. 3 (b), uniform blister formation with about 100 nm sizes is recognized. In general, the size of blisters produced in metal surfaces by helium

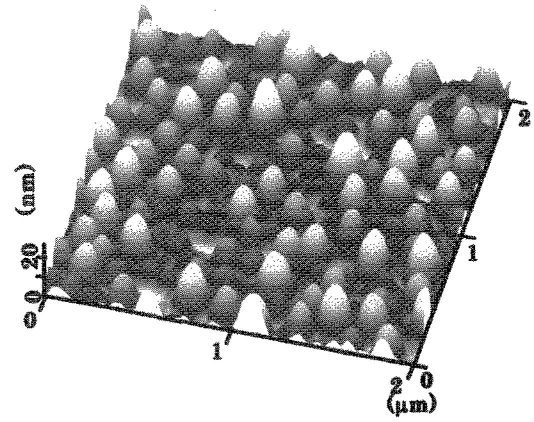

Fig. 5. AFM image (2 μm × 2 μm) of the rutile TiO_2 (100) film implanted with 3 keV helium to a fluence of 1.8 × 10^{17} ions/cm^2 at room temperature.

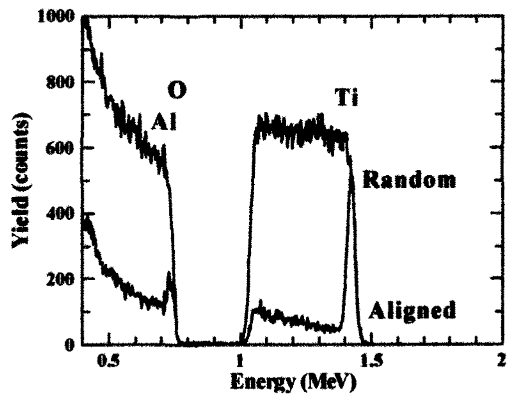

Fig. 6. 2.0 MeV $^4He^+$ RBS spectra for the rutile TiO_2 (100) film implanted with 3 keV helium to a fluence of 1.8 × 10^{17} ions/cm^2 at room temperature taken under the random and the TiO_2 <100> axial channeling condition.

implantation with a fluence of 10^{18} ions/cm^2 range at room temperature is about several μm [10]. In comparison with helium blister formation in metals, the size of blister produced in TiO_2 films is extremely small.

Figure 4 shows SEM images of the TiO_2 (100) films implanted with the helium fluence of (a) 1.8 × 10^{17} ions/cm^2 and (b) 2.3 × 10^{17} ions/cm^2. The film samples were implanted with 3 keV helium ions at room temperature. In Fig. 4 (a), one can recognize uniform helium blisters with about 100 nm size were produced without cracks in the blister surface. Further increase of helium implantation fluence up to 2.3 × 10^{17} ions/cm^2, cracks and holes are observed in the blister surface in Fig.4 (b). These results indicate that exfoliation of flakes of the TiO_2 film occurs with helium ion fluences higher than about 2 × 10^{17} ions/cm^2. In the samples made by helium implantation with 1~4 keV at room temperature, helium blisters with about 100 nm size were observed at 2~4 keV helium ion fluences higher than about 4 × 10^{16} ions/cm^2.

Figure 5 shows AFM image (2 μm × 2 μm) of the rutile TiO_2 (100) film implanted with 3 keV helium to a fluence of 1.8×10^{17} ions/cm^2 at room temperature. From AFM observation, many blisters were recognized on this sample surface. Mean radius of this blister was 125 nm, mean height was 20 nm, and areal density was about 2.5×10^9 /cm^2. The surface area of this sample increases by a factor of 1.012. This result coincides with the results of SEM observations. The mean radius of helium blister was almost the same when the helium ion fluence was changed from 5×10^{16} to 1.8×10^{17} ions/cm^2 in present experiment.

To determine the radiation-induced damage depth profile near the surface region. TiO_2 films implanted with helium ion were examined by RBS/channeling. Figure 6 illustrates 2.0 MeV $^4He^+$ RBS spectra for the rutile TiO_2 (100) film implanted with 3 keV helium to a fluence of 1.8×10^{17} ions/cm^2 at room temperature taken under the random and the axial channeling condition. The RBS spectra from unimplanted sample are shown in Fig. 1 for comparison. The RBS spectra taken under TiO_2<100> axial channeling condition in Fig. 6, the RBS yield (at 1.45 MeV) from Ti component in the TiO_2 film reaches the random level. In addition, the RBS yield from oxygen component in the film also increases. These increases of the RBS yields indicate that helium radiation-induced damage in TiO_2 film exists only near the surface region (~20 nm). This damage region corresponds to the helium blister region observed by AFM.

4. SUMMARY

We have studied the formation of helium blisters in epitaxial rutile TiO_2 (100) grown on α-Al_2O_3 (0001) as a function of the implantation fluence and energy at room temperature. The surface morphology of TiO_2 films was observed by SEM and AFM. RBS with channeling was used to determine the radiation-induced damage depth profile near the surface region. Helium blisters with ~100 nm size and ~20 nm height in TiO_2 films were observed at 2~4 keV helium ion fluences higher than 4×10^{16} ions/cm^2. Further increase of implantation fluences higher than 2×10^{17} ions/cm^2, exfoliation of flakes of the TiO_2 film was observed.

Acknowledgements

Authors with to thank Dr. M. Sugimoto of Japan Atomic Energy Research Institute for measuring the AFM images. This work was supported by a Grant in Aid for Young Scientist (B) from the Japan Society for the Promotion of Science (No.16760591).

References

[1] A. L. Linsebigler, G. Lu, J. T. Yates, Jr., Chem. Rev. **95**, 735-758 (1995).

[2] Mario Schiavello, "Heterogeneous Photocatalysis", John Wiley & Sons Ltd, (1997)

[3] Samuel Chen, M.G. Mason, H.J. Gysling, G.R. Paz-Pujalt, T.N. Blanton, T. Castro, K.M. Chen, C.P. Fictorie, W.L. Gladfelter, A. Franciosi, P.I. Cohen, J.F. Evans, J. Vac. Sci. Technol. A **11**, 2419-2429 (1993)

[4] T. Aoki, K. Maki, Q. Tang, Y. Kumagai, S. Matsumoto, J. Vac. Sci. Technol. A **15**, 2485-2488 (1997).

[5] P.A. Morris Hotsenpiller, G.A. Wilson, A. Roshko, J.B. Rothman, G.S. Rohrer, J. Crystal Growth **166**, 779-785 (1996)

[6] S. Yamamoto, T. Sumita, T. Yamaki, A. Miyashita, H. Naramoto, J. Crystal Growth **237-239**, 569-572 (2002).

[7] T. Yamaki, T. Sumita, S. Yamamoto, A. Miyashita, J. Crystal Growth **237-239**, 574-579 (2002).

[8] S. Yamamoto, T. Sumita, Sugiharuto, A. Miyashita, H. Naramoto, Thin Solid Films **401**, 88-93 (2001).

[9] Y. Matsumoto, M. Murakami, T. Hasegawa, T. Fukumura, M. Kawasaki, P. Ahmet, K. Nakajima, T. Chikyow, H. Koinuma, Appl. Surf. Sci. **189**, 344-348 (2002).

[10] P.B. Johnson, R.W. Thomson, Karen Reader, J. Nucl. Mater. **273**, 117-129 (1999).

[11]] P.B. Johnson, P.W. Gilbe, A. Markwitz, A. Raudsepp, I.W.M. Brown, Nucl. Instr. and Meth. B **166-167**, 121-127 (2000).

[12] P.B. Johnson, A. Markwitz, P.W. Gilberd, Adv. Mater. **13**, 997-1000 (2001).

[13] D.L da Silva, P.F.P Fichtner, M. Behar, A. Peeva, R. Koegler, W. Skorupa, Nucl. Instr. and Meth. B **190**, 756-760 (2002).

(Received December 24, 2004; Accepted March 25, 2005)